

Research Article

Analyses of Dynamic Behavior of Vertical Axis Wind Turbine in Transient Regime

Bacem Zghal , **Imen Bel Mabrouk**, **Lassâad Walha**,
Kamel Abboudi, and **Mohamed Haddar**

*Laboratory of Mechanical Modeling and Production (LA2MP), National School of Engineers of Sfax (ENIS),
University of Sfax, BP 1173, 3038, Tunisia*

Correspondence should be addressed to Bacem Zghal; bacem.zghal@gmail.com

Received 19 October 2018; Accepted 6 March 2019; Published 10 April 2019

Academic Editor: Emil Manoach

Copyright © 2019 Bacem Zghal et al. This is an open access article distributed under the Creative Commons Attribution License, which permits unrestricted use, distribution, and reproduction in any medium, provided the original work is properly cited.

In this paper, the dynamic behavior of a one-stage bevel gear used in vertical axis wind turbine in transient regime is investigated. Linear dynamic model is simulated by fourteen degrees of freedom. Gear excitation is induced by external and internal sources which are, respectively, the aerodynamic torque caused by the fluctuation of input wind speed in transient regime and the variation of gear mesh stiffness. In this study, the differential equations governing the system motion are solved using an implicit Newmark algorithm. In fact, there are some design parameters, which influence the performance of vertical axis wind turbine. In order to get the appropriate aerodynamic torque, the effect of each parameter is studied in this work. It was found that the rotational speed of the rotor shaft has a significant effect on the aerodynamic torque performance.

1. Introduction

Generally, vertical axis wind turbines (VAWT) have a particular architecture compared with horizontal ones. They are composed of two main parts: the blade rotor in vertical position and a mechanical gear transmission (bevel gear). Vibrations of the aerodynamic part caused by the wind speed variation are transmitted to the other part (gear transmission system) via shaft, gears, and bearing.

In literature, plenty of authors studied the aerodynamic performance of Darrieus-type of VAWT. There are two mainly approaches: momentum models and Computational Fluid Dynamics (CFD). The main benefit of momentum models is that their time of resolution is quicker than the other approach. Although the Computational Fluid Dynamics have been a useful design tool for studying the efficiency of wind turbine, the mesh generation in three-dimensional analyses needs a lot of time for the simulation. Among analytical models are researches [1–3] based on Actuator Disk and Blade-Element Method (BEM) to predict the aerodynamic torque of VAWT. In addition, computational aerodynamics methods such as multiple stream tube method

or vortex model [4–7] have been developed to optimize VAWTs performance.

The (CFD) method has been widely used in developing the characteristics of wind turbine (torque fluctuation, power output, and pressure distribution). Jiang et al. [8] employed a commercial CFD simulation for studying the effect of geometrical parameters and airfoil type on the performance of the H-Darrieus turbine with fixed pitch angle. Also, a numerical analysis of H-rotor Darrieus turbine is introduced by M.H Mohamed et al. [9]. The developing of torque fluctuation is a very important step for the reason that the instantaneous torque produced by the rotor blade is directly related to both the power generation and the gearbox vibration.

Accordingly, there are many related literatures studying bevel gears transmission. Cai-Wan Chang-jian [10] studied the nonlinear dynamic behavior of bevel gear system. Besides, Fujii et al. [11] analyzed the dynamic vibration of straight bevel gear supported by angular bearings and tapered roller. M. Li and H. Y. Hu [12] studied the dynamic analysis of a spiral bevel-gear rotor-bearing system. Y. Wang et al. [13] and J.F. Besseling [14] developed a new approach based on

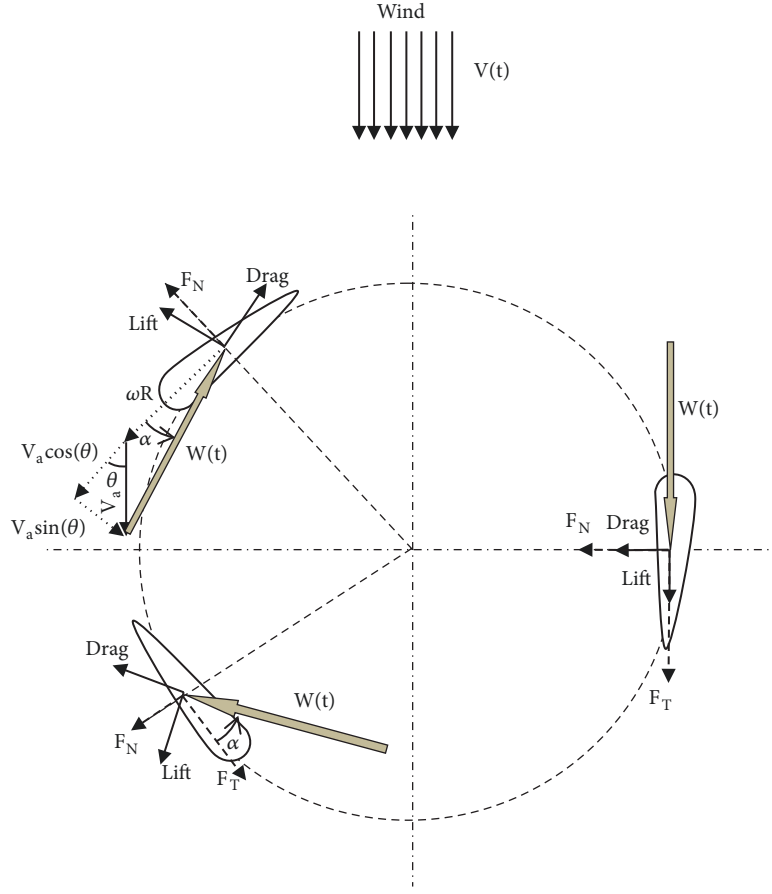


FIGURE 1: Flow velocities and forces in Darrieus wind turbine [16].

finite element theory to model bevel gear systems. Moreover, Driss Yassine et al. [15] present the model of two-stage straight bevel gear system excited with only internal excitation which is the periodic fluctuations of the gear meshes' stiffness.

In this paper, we discuss the impact of some design parameters including number of blades, turbine radius, chord length, blade length, and rotational speed on the aerodynamic torque of the H-Darrieus VAWT through analytical approach.

The main objective of the present work is to predict the dynamic behavior of the one-stage straight bevel gear system used in vertical axis wind turbine and powered by two main sources of excitation which are the optimum aerodynamic torque selected through parametrical study and the periodic variation of the gear meshes' stiffness.

2. Theoretical Modeling of VAWT Rotors

In this section, analytical investigation of aerodynamic torque of Darrieus wind turbine is established. The actuator disk theory is chosen for the aerodynamic study of the Darrieus-type wind turbine with straight blade. This theory characterizes the turbine as a disc with a discontinuity of pressure in the stream tube of air, which causes a deceleration of the wind speed. Referring to Figure 1, the relative flow velocity can be obtained as follows:

$$W = \sqrt{V_c^2 + V_n^2} \quad (1)$$

$$V_c = R\omega + V_a \cos \theta$$

$$V_n = V_a \sin \theta \quad (2)$$

$$V_a = V(t)(1 - a)$$

The angle of attack is defined as the angle between the resultant air velocity vector and the blade chord. It is expressed as follows:

$$\alpha(\theta) = \tan^{-1} \left(\frac{V_n}{V_c} \right) = \left(\frac{(1 - a) \sin \theta}{(1 - a) \cos \theta + \lambda} \right) \quad (3)$$

The value of the axial induction factor (a) can be introduced by actuator disk theory. The resultant air velocity is dependent on the induced velocity and the tip speed ratio (TSR) defined as

$$\lambda = \frac{\omega R}{V_\infty} \quad (4)$$

In this work, the induced velocity is modeled in deterministic form, as a sum of several harmonics [17]:

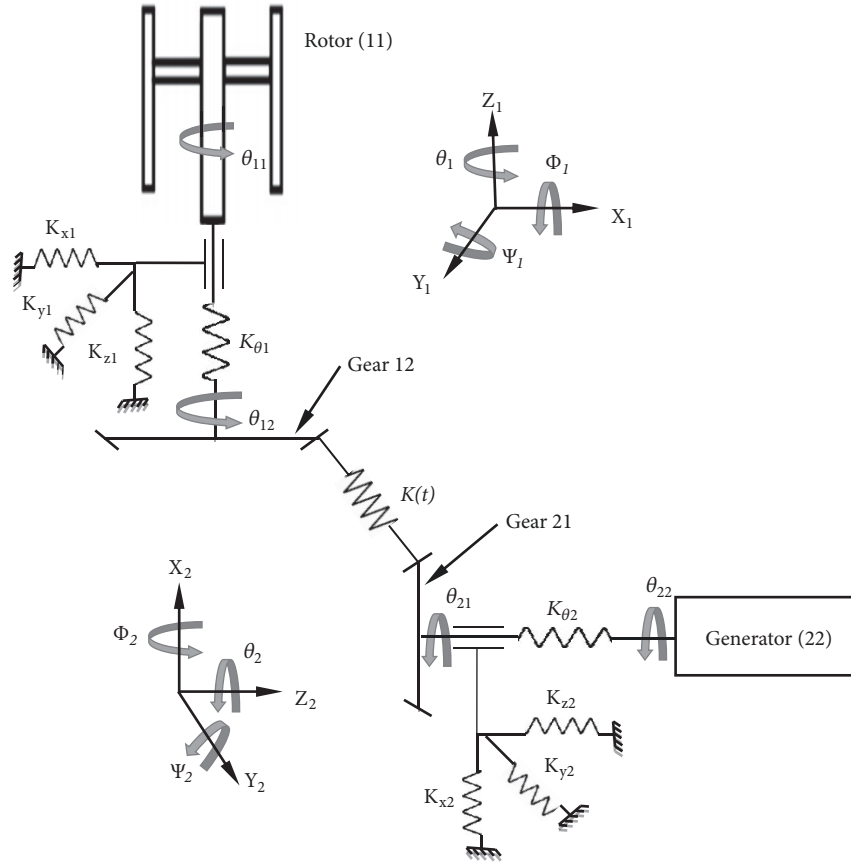


FIGURE 2: Single-stage bevel gear model.

$$V_{\infty} = 14 + 2 \sin(\omega t) - 1.75 \sin(3\omega t) + 1.5 \sin(5\omega t) - 1.25 \sin(10\omega t) + \sin(30\omega t) + 0.5 \sin(50\omega t) + 0.25 \sin(100\omega t) \quad (5)$$

The resulting aerodynamic forces in the blade can be founded by the interpolation of the lift and drag coefficients relative to the symmetrical airfoil used (NACA0018), the angle of attack, and the given Reynolds number.

The tangential and normal forces as function of the azimuth angle θ can be calculated using the blade-element theory [2].

$$F_t(\theta) = \frac{1}{2} \rho c_t W^2 h c \quad (6)$$

$$F_n(\theta) = \frac{1}{2} \rho c_n W^2 h c$$

where C_n and C_t are the normal and tangential coefficients, respectively, calculated from the lift and drag coefficients (C_L and C_D) using the same theory (blade-element momentum theory), given by following expressions:

$$C_t = C_L \sin \alpha - C_D \cos \alpha \quad (7)$$

$$C_n = C_L \cos \alpha + C_D \sin \alpha$$

The average torque produced by the rotor (n blades) is generated from the average tangential force acting on one blade:

$$T(\theta) = n \frac{1}{2\pi} \int_0^{2\pi} F_t(\theta) d\theta R \quad (8)$$

The average torque coefficient is calculated by

$$C_T = \frac{T(\theta)}{0.5 \rho V_{\infty}^2 A R} \quad (9)$$

Finally, the power coefficient C_p is estimated from the average torque coefficient:

$$C_p = \lambda C_T \quad (10)$$

3. Theoretical Modeling of the One-Stage Bevel Gear System

This part investigates the studying of the dynamic behavior of bevel gear system used in vertical axis wind turbine. The main excitations of the one-stage bevel gear system are the selected aerodynamic torque estimated through parametrical analysis in addition to the internal mesh stiffness excitation.

The dynamic model of single-stage bevel gear is presented by fourteen degrees of freedom (see Figure 2). This model

includes two blocks where the first block is constituted by the Darrieus rotor modeled by the mass (11) linked to the wheel (12) via a first shaft with torsional rigidity $K\theta_1$; this block is supported by a bearing.

The second block includes the pinion (21), the second shaft with torsional rigidity $K\theta_2$, and the generator modeled by a mass (22). It is also supported by a bearing. The wheel (12) is connected to the pinion (21) via teeth mesh stiffness. The bearings are modeled by linear springs acting on the lines of action. The mesh stiffness characterizes the elastic deformations managing the relative positions of the two gear wheels; it can be modeled by the mesh stiffness $k(t)$.

The proposed dynamic model is modeled by the generalized coordinate vector $\{q\}$:

$$\{q(t)\} = [x_1, y_1, z_1, x_2, y_2, z_2, \phi_1, \psi_1, \phi_2, \psi_2, \theta_{11}, \theta_{12}, \theta_{21}, \theta_{22}]^T \quad (11)$$

$\{x_i, y_i, z_i\}$ are the linear displacements of bearing in each block.

$\{\phi_i, \psi_i, \theta_{1i}, \theta_{2i}\}$ are the angular displacement of bearing and wheel ($i=1,2$).

The equations of motion describing the dynamic behavior of the model are established using the formalism of Lagrange for each degree of freedom of the system.

$$[M] \{\ddot{q}\} + [C] \{\dot{q}\} + ([K_s] + [K(t)]) \{q\} = \{F(t)\} \quad (12)$$

The total mass matrix is defined by

$$[M] = \begin{bmatrix} [M_L] & 0 \\ 0 & [M_A] \end{bmatrix} \quad (13)$$

$$[M_L] = \text{diag} [m_1, m_1, m_1, m_2, m_2, m_2] \quad (14)$$

$$[M_A] = \text{diag} [I_{11x} + I_{12x}, I_{11y} + I_{12y}, I_{21x} + I_{22x}, I_{21y} + I_{22y}, I_{11}, I_{12}, I_{21}, I_{22}] \quad (15)$$

$[K_s]$ is the average stiffness matrix of the structure

$$[K_s] = \begin{bmatrix} [K_p] & 0 \\ 0 & [K_\Theta] \end{bmatrix} \quad (16)$$

$$\text{where: } [K_p] = \text{diag} [k_{x1}, k_{y1}, k_{z1}, k_{x2}, k_{y2}, k_{z2}] \quad (17)$$

$$[K_\Theta]$$

$$= \begin{bmatrix} k_{\phi_1} & 0 & 0 & 0 & 0 & 0 & 0 & 0 \\ 0 & k_{\psi_1} & 0 & 0 & 0 & 0 & 0 & 0 \\ 0 & 0 & k_{\phi_2} & 0 & 0 & 0 & 0 & 0 \\ 0 & 0 & 0 & k_{\psi_2} & 0 & 0 & 0 & 0 \\ 0 & 0 & 0 & 0 & k_{\theta_1} & -k_{\theta_1} & 0 & 0 \\ 0 & 0 & 0 & 0 & -k_{\theta_1} & k_{\theta_1} & 0 & 0 \\ 0 & 0 & 0 & 0 & 0 & 0 & k_{\theta_2} & -k_{\theta_2} \\ 0 & 0 & 0 & 0 & 0 & 0 & -k_{\theta_2} & k_{\theta_2} \end{bmatrix} \quad (18)$$

The mesh stiffness matrix can be defined by

$$[K(t)] = k(t) \langle L \rangle^T \cdot \langle L \rangle \quad (19)$$

$[k(t)]$ is the total meshing stiffness of the gear pair. Sha Wei et al. [18] have expressed the total meshing stiffness of the gear pair by a periodic excitation decomposed on Fourier series.

The tooth deflection following the line of action is defined by

$$\delta(t) = \langle L \rangle \cdot \{q(t)\} \quad (20)$$

$$\{L\} = \{c_1, c_2, c_3, c_4, c_5, c_6, c_7, c_8, c_{10}, c_{11}, 0, c_9, c_{12}, 0\} \quad (21)$$

The components of the tooth deflection are presented in Table 1.

The load vector can be written as

$$\{F(t)\} = \{0 \ 0 \ 0 \ 0 \ 0 \ 0 \ 0 \ 0 \ 0 \ 0 \ T(t) \ 0 \ 0 \ -R_T(t)\}^T \quad (22)$$

$T(t)$ and $R_T(t)$ are the aerodynamic torque produced by the rotor and the resisting torque, respectively. $[C]$ is the proportional damping matrix

$$[C] = 0.05 [M] + 10^{-5} [\tilde{K}] \quad (23)$$

where $a_{12} = \sin(\delta_{b12})$, $b_{12} = \cos(\delta_{b12})$, $a_{21} = \sin(\delta_{b21})$, and $b_{21} = \cos(\delta_{b21})$.

δ_{bji} and r_{2i} are the half-angle of the base circle of bevel gear (i) of the block (j) and the radius of the sphere which contains two bevel gears, (12) and (21), respectively ($r_{12} = r_{21}$).

The angles δ_b and u describe the different parameters of the bevel gear [18].

4. Influence of Rotor Configuration on Turbine Performance

The main purpose of this study is to investigate the effect of different design parameters (blade chord, number of blades, and radius turbine) on the aerodynamic torque evaluation of H-Darrieus turbine, using analytical approach.

The solidity σ is defined as an important nondimensional parameter, which influences the self-starting abilities and determines the applicability of the momentum models. The turbine is able to self-start for high solidity ($\sigma \geq 0.4$) [2]. For straight bladed VAWTs, the solidity is calculated by

$$\sigma = \frac{nc}{R} \quad (24)$$

In order to study the dynamic behavior of bevel gear system used on vertical axis wind turbine and powered by the aerodynamic torque in transient regime in addition to the periodic variations of mesh stiffness, we used numerical simulation based on implicit method of Newmark.

The parameters of the bevel gear transmission are presented in Table 2. Specifications of the vertical axis wind turbine are shown in Table 3.

TABLE 1: Components of the tooth deflection.

c_1	$b_{12} \sin(a_{12}u_{12})$
c_2	$a_{12} \cos u_{12} \sin(a_{12}u_{12}) - \sin u_{12} \cos(a_{12}u_{12})$
c_3	$a_{12} \sin u_{12} \sin(a_{12}u_{12}) + \cos u_{12} \cos(a_{12}u_{12})$
c_4	$b_{21} \sin(a_{21}u_{21})$
c_5	$a_{21} \cos u_{21} \sin(a_{21}u_{21}) - \sin u_{21} \cos(a_{21}u_{21})$
c_6	$a_{21} \sin u_{21} \sin(a_{21}u_{21}) + \cos u_{21} \cos(a_{21}u_{21})$
c_7	$c_2 r_{12} b_{12} \cos(a_{12}u_{12}) - c_1 r_{12} (a_{12} \cos u_{12} \cos(a_{12}u_{12}) + \sin u_{12} \sin(a_{12}u_{12}))$
c_8	$c_1 r_{12} (a_{12} \sin u_{12} \cos(a_{12}u_{12}) - \cos u_{12} \sin(a_{12}u_{12})) - c_3 r_{12} b_{12} \cos(a_{12}u_{12})$
c_9	$c_3 r_{12} (a_{12} \cos u_{12} \cos(a_{12}u_{12}) + \sin u_{12} \sin(a_{12}u_{12})) - c_2 r_{12} (a_{12} \sin u_{12} \cos(a_{12}u_{12}) + \cos u_{12} \sin(a_{12}u_{12}))$
c_{10}	$c_4 r_{21} (a_{21} \cos u_{21} \cos(a_{21}u_{21}) + \sin u_{21} \sin(a_{21}u_{21})) - c_5 r_{21} b_{21} \cos(a_{21}u_{21})$
c_{11}	$c_5 r_{21} (a_{21} \sin u_{21} \cos(a_{21}u_{21}) - \cos u_{21} \sin(a_{21}u_{21})) - c_6 r_{21} b_{21} \cos(a_{21}u_{21})$
c_{12}	$-c_6 r_{21} (a_{21} \cos u_{21} \cos(a_{21}u_{21}) + \sin u_{21} \sin(a_{21}u_{21})) + c_5 r_{21} (a_{21} \sin u_{21} \cos(a_{21}u_{21}) - \cos u_{21} \sin(a_{21}u_{21}))$

TABLE 2: Parameters of the studied bevel gear system.

Teeth number	18 / 45
module(m)	0.004
Bearing stiffness (N/m)	$k_{x1} = k_{y1} = k_{x2} = k_{y2} = 2 \cdot 10^8$
Torsional stiffness(N/rd/m)	$k_{z1} = k_{z2} = 4.10^8$
Pressure angle	$k_{\theta1} = k_{\theta2} = 310^8$
Contact ratio	$\alpha = 20^\circ$
Average mesh stiffness(N/m)	$\varepsilon_\alpha = 1.56$
Density (42CrMo4)	$K_{moy} = 410^8$
	7860 kg/m^3

TABLE 3: Wind turbine specification.

Type	Straight blade Darrieus
Airfoil profile	NACA0018
Airfoil chord(mm)	480
Blade length (m)	3.66
Turbine diameter (m)	4
Blade number	3
Speed of rotor (tr/min)	50

The number of blades (n) is an important factor that influences the torque produced. It is well known that a bigger number of blades give rise to the solidity and produce a global torque with small fluctuation. However, increasing the number of blades lead to increase in the turbine drag by increasing the number of connecting shafts. Figure 3 shows the effect of the blade number on the torque in full revolution for a case where the radius and blade chord are maintained constant while the number of blades changes. As can be deduced, 3-bladed VAWT perform more efficient than 2 and 4 bladed turbines.

In Figure 4 the effect of blade chord on the torque fluctuation is presented. We remark that torque magnitude increases when the chord length increases. Also, blades with smaller chords require a bigger tip speed ratio to achieve a maximum torque so the selection of chord length affects the self-starting behavior of Darrieus turbine.

As can be assumed from the torque equation (8), the rotor radius and the blade length have a major contribution in

the torque behavior of VAWT turbine. An increase in radius turbine and blade height advances the instantaneous torque as shown in Figures 5 and 6.

Figure 7 shows the total torque evolution versus azimuth angle generated for a complete revolution with different rotation speed. It can be observed that the torque increases considerably with the increase of the rotation speed. Also, the torque fluctuation becomes positive when the rotation speed reaches 178 rev/min. However, for a case of 50 rev/min and 177 rev/min the instantaneous torque presents some fluctuation with negative magnitude which can explain the no self-starting of NACA0018 airfoil.

As shown in Figures 8 and 9 rising wind speed from 8 to 14 m/s significantly affects the torque which increases considerably. The cyclic distribution of total torque at higher rotational speed ($N=180$ rev/min) and at small rotational speed ($N=50$ rev/min) is observed at the same wind speed of 14 m/s.

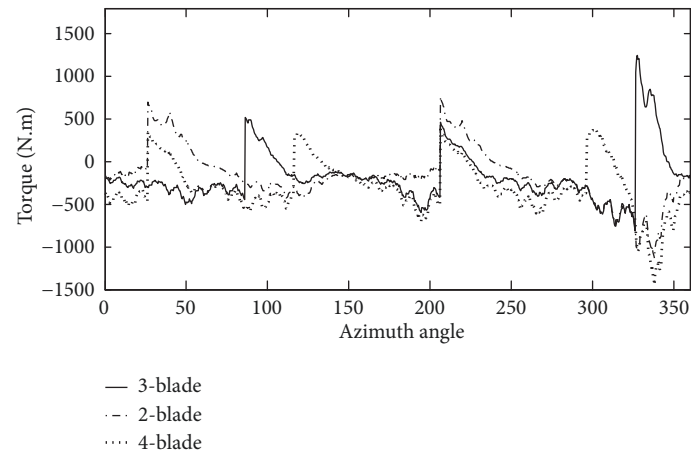


FIGURE 3: Effect of blades number on the torque.

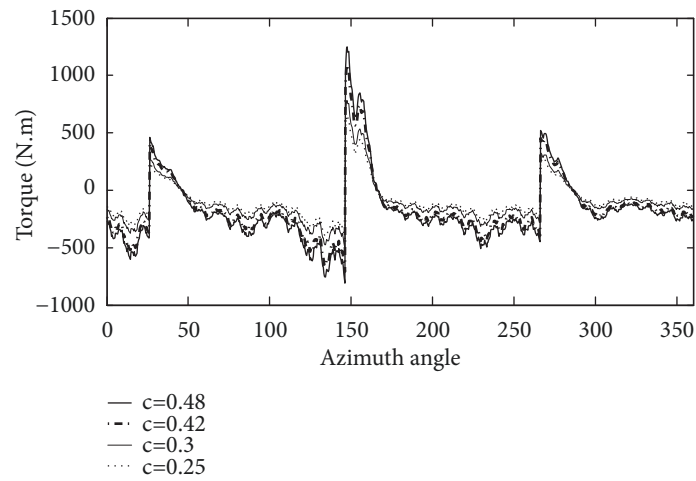


FIGURE 4: Effect of blade chord on the torque.

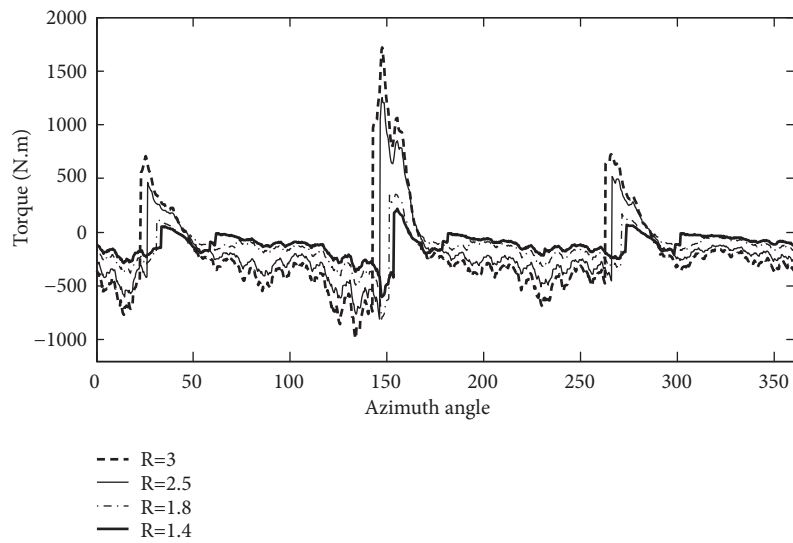


FIGURE 5: Effect of radius turbine on the torque.

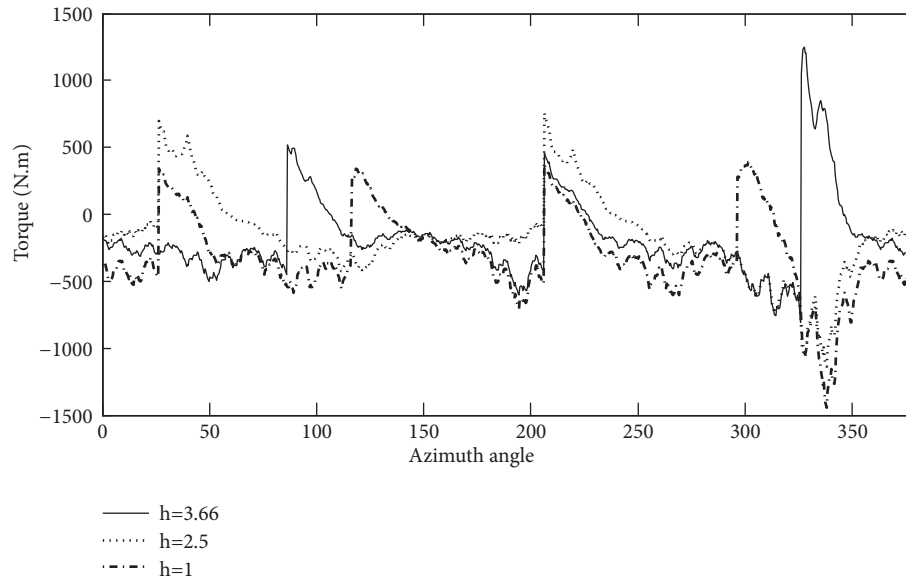


FIGURE 6: Effect of blade height on the torque.

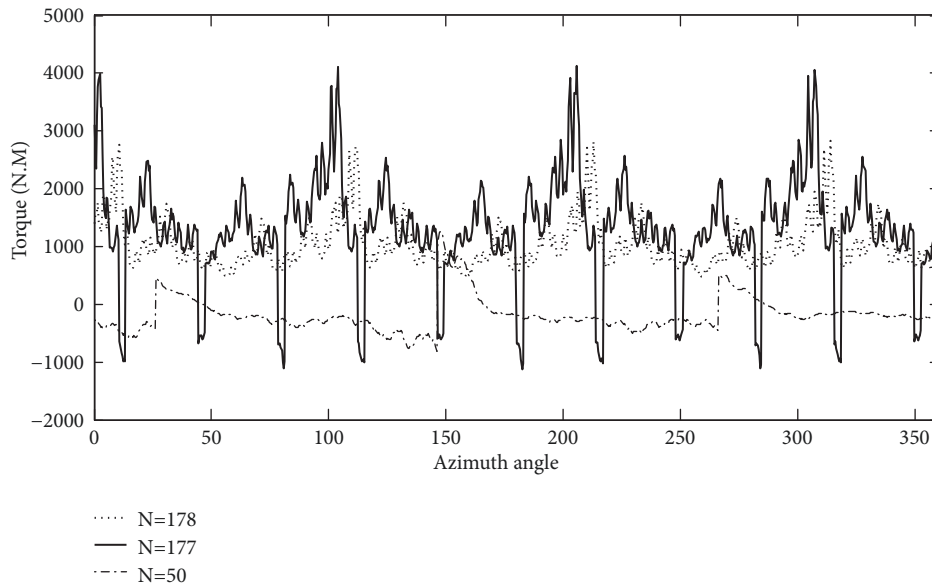


FIGURE 7: Effect of rotation speed on the torque.

We clearly see only positive fluctuation of the aerodynamic torque at $N=180$ tr/min; however, this torque presents negative oscillation at small rotational speed ($N=50$ tr/min) at fixed wind speed of 14 m/s. Consequently, we conclude the most favorable speed excitation of the considerable Darrieus rotor that corresponds to wind velocity of 14 m/s and rotational speed of 180 tr/min which respects the condition of positive torque evolution.

5. Conclusion

This paper presents a three-dimensional model of one-stage straight bevel gear system used in vertical axis wind turbine. Aerodynamic torque fluctuation and periodic oscillation of the gear meshes' stiffness are the main sources of excitation for the bevel gear system.

Influence of geometrical parameters of Darrieus rotor has been done in order to select the appropriate parameters. The optimization process has been carried out on the effect of each parameter on the aerodynamic torque produced.

It was found that the aerodynamic torque increases when the chord, the radius, and the height of VAWT rise. However, the best performance is detected for 3-bladed VAWT. Finally, the most significant parameter that affects the aerodynamic torque is the rotation speed of the rotor shaft.

Nomenclature

- a: Axial induction factor
- A: Turbine swept area
- c: Chord (m)

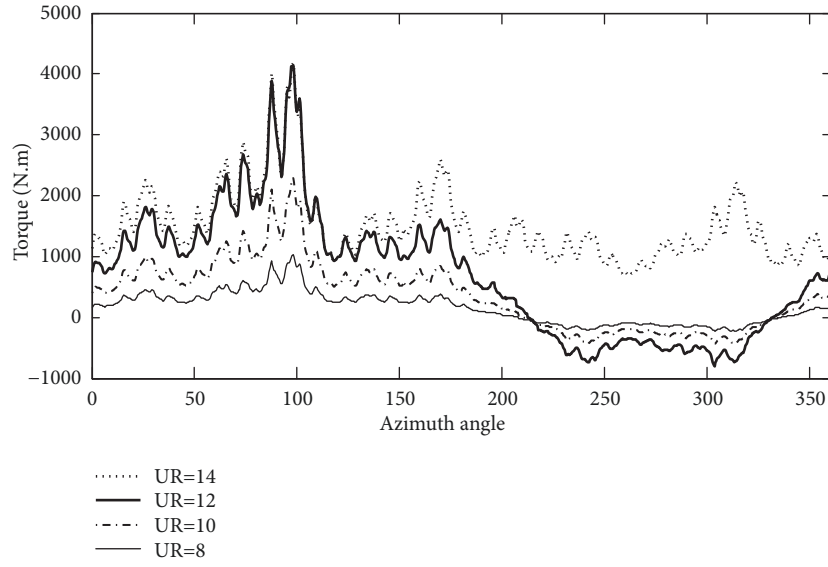


FIGURE 8: Effect of wind speed on the torque (N=180tr/min).

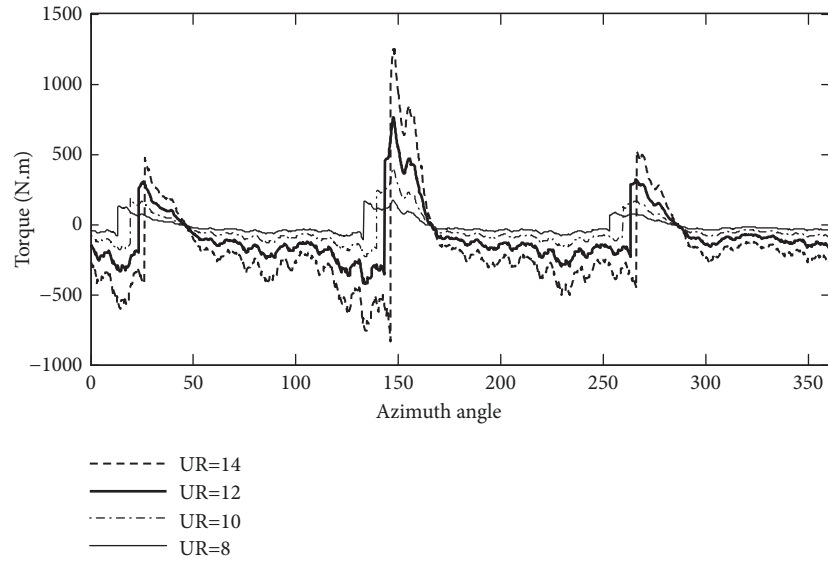


FIGURE 9: Effect of wind speed on the torque (N=50tr/min).

$[C]$: Proportional damping matrix

C_t : Tangential force coefficient

C_n : Normal force coefficient

C_T : Average torque coefficient

C_p : Power coefficient

C_L, C_D : Lift and drag coefficients

F_t : Tangential force

F_n : Normal force

$\{F(t)\}$: External excitation force

h : Blade height (m)

I_{ij} : Moment of inertia of the wheel j of block i

I_{ijx}, I_{ijy} : Diametrical moment of wheel j of block i respectively following the X- and Y-axes

$k(t)$: Gear mesh of stiffness

$[K(t)]$: Time stiffness matrix of the gear mesh fluctuation

$[K_s]$: Stiffness matrix of the average structure

$k_{\theta i}$: Shafts torsional stiffness

K_{xi}, k_{yi}, k_{zi}

$K_{\Phi i}$ and $K_{\psi i}$: Bending and traction-compression bearing stiffness

$[M]$: Mass matrix

m_i : Mass of block i

$\langle L \rangle$: Vector of geometric parameters of the dynamic model

n : Blade number

N : Rotational speed of the rotor (tr/min)

$\{q(t)\}$: Generalized coordinate vector

R : Radius of the wind turbine (m)

$R_T(t)$: Resisting torque

$T(t)$: Aerodynamic torque

$V(t)$:	Wind free stream velocity (m/sec)
V_a :	Induced velocity
V_c, V_n :	Chordal velocity component and the normal velocity component, respectively
W :	Relative flow velocity
θ :	Azimuth angle
ω :	Angular velocity (rad/sec)
ρ :	Air density [kg/m^3]
λ :	Tip speed ratio
$\delta(t)$:	Relative displacement of the contact point along the line of action
δ_{bij}, u_{ij} :	Geometric angle of bevel gear
$\{x_i, y_i, z_i\}$:	Bearing displacements in each blocs ($i=1:2$)
$\{\phi_i, \psi_i\}$:	Angular displacement of the bearing following X and Y, respectively
$\{\theta_{1i}, \theta_{2i}\}$:	Angular displacement of wheel and gear following Z direction ($i=1:2$)
σ :	Solidity
$\alpha(\theta)$:	Angle of attack.

Data Availability

All results are obtained by simulation with Matlab.

Conflicts of Interest

The authors declare that they have no conflicts of interest.

References

- [1] R. E. Wilson, "Wind-turbine aerodynamic," *Journal of Industrial Aerodynamics*, pp. 357–372, 1980.
- [2] C. Javier, *Small-scale vertical axis wind turbine design. Bachelors Thesis*, Aeronautical Engineering, Tampere University of Applied Sciences, 2011.
- [3] D. Prathamesh and C. L. Xian, "Numerical study of giromill-type wind turbines with symmetrical and non-symmetrical airfoils," *Journal of Science and Technology*, 2013.
- [4] J. H. Strickland, "The Darrieus turbine: a performance prediction model using multiple streamtube," *Sandia Laboratories Report. SAND*, pp. 75–431, 1975, United States of America.
- [5] I. paraschivoiu, "Double-multiple stream tube model for studying vertical-axis wind turbines," *Journal of Propulsion and Power*, vol. 4, no. 4, pp. 370–377, 1988.
- [6] H. Beri and Y. Yao, "Double multiple stream tube model and numerical analysis of vertical axis wind turbine," *International Journal of Energy and Power Engineering*, vol. 3, no. 3, pp. 262–270, 2011.
- [7] L. Wang, L. Zhang, and N. Zeng, "A potential flow 2-D vortex panel model: applications to vertical axis straight blade tidal turbine," *Energy Conversion and Management*, vol. 48, no. 2, pp. 454–461, 2007.
- [8] Z.-C. Jiang, Y. Doi, and S.-Y. Zhang, "Numerical investigation on the flow and power of small-sized multi-bladed straight Darrieus wind turbine," *Journal of Zhejiang University SCIENCE A*, vol. 8, no. 9, pp. 1414–1421, 2007.
- [9] M. H. Mohamed, A. M. Ali, and A. A. Hafiz, "CFD analysis for H-rotor Darrieus turbine as a low speed wind energy converter," *Engineering Science and Technology, an International Journal*, vol. 18, no. 1, pp. 1–13, 2015.
- [10] C.-W. Chang-Jian, "Nonlinear dynamic analysis for bevel-gear system under nonlinear suspension-bifurcation and chaos," *Applied Mathematical Modelling*, vol. 35, no. 7, pp. 3225–3237, 2011.
- [11] M. Fujii, Y. Nagasaki, and M. Nohara Trauchi, "Effect of bearing on dynamic behavior of straight bevel gear train," *Transactions of the Japan Society of Mechanical Engineers A*, vol. 61, pp. 234–238, 1995.
- [12] M. Li and H. Y. Hu, "Dynamic analysis of a spiral bevel-gear rotor-bearing system," *Journal of Sound and Vibration*, vol. 259, no. 3, pp. 605–624, 2003.
- [13] Y. Wang, W. Zhang, and H. Cheung, "A finite element approach to dynamic modeling of flexible spatial compound bar-gear systems," *Mechanism and Machine Theory*, vol. 36, no. 4, pp. 469–487, 2001.
- [14] J. F. Besseling, "Derivatives of deformation parameters for bar elements and their use in buckling and postbuckling analysis," *Computer Methods in Applied Mechanics and Engineering*, vol. 12, pp. 97–124, 1977.
- [15] D. Yassine, H. Ahmed, W. Lassaad, and H. Mohamed, "Effects of gear mesh fluctuation and defaults on the dynamic behavior of two-stage straight bevel system," *Mechanism and Machine Theory*, vol. 82, pp. 71–86, 2014.
- [16] M. Islam, D. Ting, and A. Fartaj, "Aerodynamic models for Darrieus-type straight-bladed vertical axis wind turbines," *Renewable & Sustainable Energy Reviews*, vol. 12, no. 4, pp. 1087–1109, 2008.
- [17] A. Mirecki, *Comparative study of energy conversion system dedicated to a small wind turbine [Ph.D. thesis]*, Polytechnic National Institute, Toulouse, France, 2005.
- [18] S. Wei, J. Zhao, Q. Han, and F. Chu, "Dynamic response analysis on torsional vibrations of wind turbine geared transmission system with uncertainty," *Journal of Renewable Energy*, vol. 78, pp. 60–67, 2015.

